УДК 551.461

© *О. О. Трусенкова*[1]*, *В. Б. Лобанов*[1], *Е. В. Примачев*[2]

[1]Тихоокеанский океанологический институт им. В.И. Ильичева Дальневосточного отделения РАН, 690041, ул. Балтийская, 43, г. Владивосток, Россия
[2]Департамент Росгидромета по ДФО, 680000, ул. Ленина, д. 18, г. Хабаровск
*E-mail: trolia@poi.dvo.ru

# ВНУТРИГОДОВАЯ ИЗМЕНЧИВОСТЬ УРОВНЯ ЯПОНСКОГО МОРЯ В СЕВЕРО-ЗАПАДНОЙ ПРИБРЕЖНОЙ ЗОНЕ

Статья поступила в редакцию 07.09.2020, после доработки 11.12.2020

По измерениям за 2010–2015 гг. на прибрежных гидрометеорологических станциях, расположенных на открытом побережье Приморского края (Преображение, Рудная Пристань, Сосуново), проанализирована изменчивость уровня моря в прибрежной зоне северо-западной части Японского моря. На основе вейвлет-преобразования были впервые обнаружены нестационарные колебания на масштабах 120–130 и 70–80 сут. Также были зарегистрированы ранее выявленные квазидвухлетние, годовые, полугодовые, приливные (суточные и полусуточные) и инерционные колебания уровня моря. Оценка интенсивности динамических процессов была выполнена на основе мощности вейвлет-спектра уровня моря, осредненной в диапазоне 8–40 сут, соответствующему временам жизни синоптических и мезомасштабных вихрей в этом районе. Установлено, что эта интенсивность изменяется на квазидвухлетнем, годовом, 120–130- и 70–80-суточном масштабах, т. е. изменчивость уровня моря с периодами 120–130 и 70–80 сут можно связать с динамическими процессами. До апреля-июня 2014 г. внутригодовая изменчивость была, в целом, синфазной в районах трех гидрометеорологических станций, но она стала рассогласованной в конце периода наблюдений.

**Ключевые слова:** уровень моря, гидрометеорологическая станция, прибрежная зона, Японское море, внутригодовая изменчивость, вейвлет-преобразование.

© *O. O. Trusenkova*[1]*, *V. B. Lobanov*[1], *E. V. Primachev*[2]

[1]V.I. Il'ichev Pacific Oceanological Institute, Far Eastern Branch of RAS, 690041, Baltiyskaya Str., 43, Vladivostok, Russia
[2]Roshydromet Department for the Far Eastern Federal District, Khabarovsk, Russia
*E-mail: trolia@poi.dvo.ru

# SEA LEVEL INTRA-ANNUAL VARIABILITY IN THE COASTAL NORTHWESTERN PART OF THE SEA OF JAPAN

Received 07.09.2020, in final form 11.12.2020

Sea level variability was analyzed using tide gauge data for 2010–2015 from three Russian hydrometeorological stations located along the open coastline in the Primorye (Liman) Current zone, in the northwestern part of the Sea of Japan. Based on wavelet transform, non-stationary sea level oscillations on the 120–130 and 70–80 days timescales were detected for the first time in the northwestern part of the Sea of Japan. Quasi-biennial, annual, semiannual, tidal diurnal and semi-diurnal, and inertial sea level oscillations found in earlier studies were also registered. The intensity of dynamic processes was estimated from the wavelet spectral power averaged in the 8–40 days range corresponding to lifetimes of mesoscale/submesoscale eddies in the Primorye Current zone. The variability timescales of this intensity were found to match that of the sea level (more precisely, the timescales of 70 days and longer). This implies that the 120–130 and 70–80 days sea level variability can be related to dynamic processes. At the three coastal stations, more than 200 km distant from each other, this kind of variability was in phase before mid 2014 and then diverged.

**Key words:** sea level, tide gauge, Sea of Japan, coastal zone, intra-annual variability, wavelet transform.

## 1. Introduction

Rapid economic development and increasing anthropogenic pressure call for oceanographic research of the coastal areas in the Russian Far-Eastern marginal seas, in particular, for analyses of the sea level variability, an

Ссылка для цитирования: *Трусенкова О.О.*, *Лобанов В.Б.*, *Примачев Е.В.* Внутригодовая изменчивость уровня Японского моря в северо-западной прибрежной зоне // Фундаментальная и прикладная гидрофизика. 2021. Т. 14, № 1. С. 54–62. doi: 10.7868/S2073667321010056

For citation: *Trusenkova O.O.*, *Lobanov V.B.*, *Primachev E.V.* Sea Level Intra-Annual Variability in the Coastal Northwestern Part of the Sea of Japan. *Fundamentalnaya i Prikladnaya Gidrofizika*. 2021, 14, 1, 54–62. doi: 10.7868/S2073667321010056

essential climate variable and an indicator of dynamic processes in the ocean. Using coastal tide gauge and satellite altimetry data for the Sea of Japan, sea level fluctuations of different origins on various timescales were revealed in earlier studies.

As for the seasonal variation in the Sea of Japan, the sea level rises in the warm season and drops in the cold season, which can be attributed to steric effects, mostly due to temperature changes (see original results and review in [1]). This finding was confirmed later with the use of longer tide gauge records [2] and it was expanded to the entire sea, based on altimetry data [3, 4]. The seasonal variation of surface currents was revealed from altimetry data: the strengthening of the large-scale meridional sea level gradient resulted in the circulation intensification in late summer [5] or in autumn [4] and the gradient slackening resulted in circulation weakening in late winter [4, 5]. These changes were explained by steric effects due to the seasonal variation of water transport in the Korea Strait and differential surface cooling.

Sea level variability was also studied on timescales longer than one year. Using altimetry data, quasi-biennial (QB) fluctuations were revealed, first in the southern part of the Sea of Japan where they were related to wind forcing [6] and to the path variations of the Tsushima Warm Current [7] and later in the entire sea [3, 4]. That they could occur simultaneously in the entire sea, intensifying in the periods when the transport in the Korea Strait increased, implies a relationship with transport imbalance in the straits [4]. Using the decadal record of altimetry data and long-term tide gauge and cruise data, interannual and decadal sea level variability in the southern part of the Sea of Japan was studied and found to be related to steric effects due to changes in properties of water coming through the Korea Strait [8–10]. The 12–13 year fluctuations occurring simultaneously in the entire sea were considered to be related to the transport variations in the Korea Strait [11]. Linear trends were repeatedly estimated, using the extended altimetry record, and sea level rise was detected, in line with the findings for the World Ocean. For the first 9–10 years of the altimetry record (from October 1992) the rising rate in the southern part of the Sea of Japan was twice as large as the global mean rate [3, 9]. With the record extension, the rising rate showed a decrease and eventually became almost equal to the global mean rate [10, 11]. Long tide gauge records (from 1950s) show oscillatory rather than trend-like sea level patterns in the Japan Sea [3, 10].

Although tides are not strong in the part of the Sea of Japan, they are still non-negligible and are mostly of the mixed character [12, 13]. Semi-diurnal tides prevail in the Korea Strait, while the semi-diurnal to diurnal tide ratio decreases northward and again increases in the Tatarsky Strait where the semi-diurnal tides prevail [12, 14] (see fig. 1 for location of the straits). Using tide gauge data, it was shown that storm surges are the most frequent in August — September and that they strengthen from the south to the north [13–15].

The range between the atmospheric synoptic and annual timescales includes sea level variability related to dynamic processes in the Sea of Japan. Semiannual fluctuations were analyzed from tide gauge [2] and altimetry [3, 4] data and were found to be related to the circulation changes forced by wind in the western [16] and northern [17] sea. From altimetry data, the bi-monthly [3, 18] and 100–150 day, simultaneous in the entire southern part of the sea [7], oscillations were detected. The latter were explained by high-frequency fluctuations of water transport in the Korea Strait [7]. The intra-annual variability of sea level was also related to progressive and standing waves [3]. However, less attention has been paid to the northwestern part of the Sea of Japan, in particular, to the coastal area where a variety of dynamic processes can develop on multiple timescales.

The Primorye (Liman) Current is a cold boundary current that flows southwestward along the shelf edge and slope in the northwestern part of the Sea of Japan. Recent studies have demonstrated a complex water dynamics in the Primorye Current area [19–22]. Boundary waves propagate along the continental slope, while anticyclonic shear eddies can develop between the current and coast, providing an efficient cross-shelf water exchange. The transformed subtropical water can be transported there by mesoscale structures (eddies and jets). The sources of the warm water are the northward flowing Tsushima Current in the eastern area off the Japanese coast and the East Korea Warm Current in the southwestern area off the Korea Peninsula. Mesoscale and submesoscale structures have a considerable impact on the coastal sea level, with substantial variability; their lifetimes vary from a few days to several months and longer [19, 21, 22]. To reveal the statistical properties of eddies, automated procedures were applied to the altimetry data in many areas of the World Ocean [23], in particular in the southern part of the Sea of Japan [24]. Statistical methods were frequently applied for the sea level analysis in the Sea of Japan [3–5, 7, 17] but the resolution of altimetry data was too coarse for capturing the small-scale processes in the northwestern coastal zone. Tide gauge data with high temporal resolution seems more appropriate, while timescales of non-stationary fluctuations can be elucidated with the use of wavelet transform.

This study was focused on the intra-annual variations of sea level in the coastal northwestern part of the Sea of Japan. The analysis was based on tide gauge measurements from three hydrometeorological stations situated at the open coastline in the settlements of Preobrazhenie, Rudnaya Pristan’ and Sosunovo (fig. 1; hereafter referred to as stations P, R, and S, respectively.) These stations are located within the Primorye Current zone but their hydrographic regimes are considerably different. The northernmost station S is dominated by the influence of the Primorye Current, while the stations R and P are affected by the warm water advection, as discussed above.

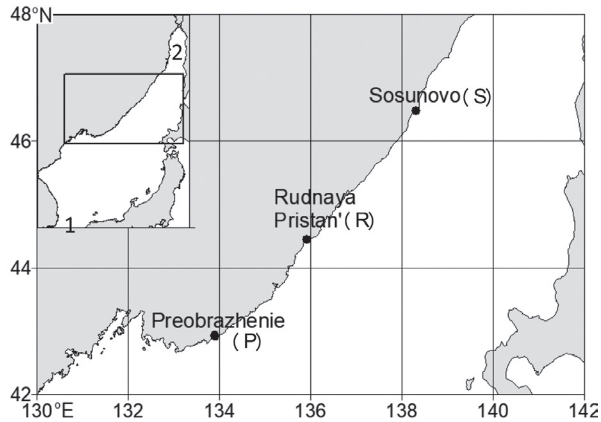


**Fig. 1.** Names and locations of tide gauges used in this study. The Korea and Tatarsky Straits are marked by numbers 1 and 2, respectively.

## 2. Data and methods

The analysis was based on sea level measurements at the hydrometeorological stations P (42.88° N, 133.89° E), R (44.36° N, 135.84° E), and S (46.54° N, 138.36° E) (fig. 1). Measurements at these stations were made for 2240 days from January 1, 2010, through February 18, 2016, by means of Aanderaa pressure sensors. There were numerous sensor failures and data gaps at the beginning of the record at the station S, therefore, only data for May 12, 2012 — February 18, 2016 (1371 days) were used for further analysis.

Measurements were made every minute, then were averaged for every hour by sensor chip processors and the hourly data were finally collected. The primary processing included the removal of erroneous data and accounting for the reference level shifts after sensor tunings or repairs. The sea levels measured at the different stations were attributed to different reference frames. For comparability, sea level anomalies (SLA) were computed and normalized by the root-mean-square values equal to 13.3, 15.2 and 12.3 cm for stations P, R and S, respectively (fig. 2). According to the Aanderaa technical documentation, the stochastic error is equal to 0.01 % of the measurement range. With the actual range about 400 cm, the error is equal to 0.4 mm. However, it was shown that systematic errors were mostly generated by the drift in pressure sensors, which did not exceed 0.8 cm/year [25]. So, the possible drift of 5 cm for 6 years and 49 days was accepted as the systematic error of every 1 min measurement. As data were averaged to 1 hour, the error was reduced by $1/60^{1/2}$, i. e. it became equal to 0.64 cm. The data were additionally averaged to 2 hours (see below), reducing the error further to become equal to 0.45 cm. SLA are further analyzed if only they exceed this value. As the numbers of degrees of freedom for the applied SLA time series were estimated as 20–22, the correlations, statistically significant at the 95 % confidence level, should exceed 0.43–0.47, according to the Fisher criterion.

There were gaps in the data with 1 hour resolution due to the gaps in the original 1 min measurements. Data at station P were the most complete, with just 12 gaps with a duration of no more than 3 hours, a 6-hour gap and a 2-day gap. In the data at station R there were 6 gaps of no more than 3 hours, a 5-hour gap and a two-week gap in 2014, spanning from August 15 through August 30 (1687–1702th days from the beginning of the record). The station S data featured several dozen gaps of no more than 3 hours, mostly in 2014, 7 gaps of 3–12 hours, 2 gaps of 12–24 hours and a two-week gap in 2014, from June 30 through July 15 (1641–1656th days from the beginning of the record).

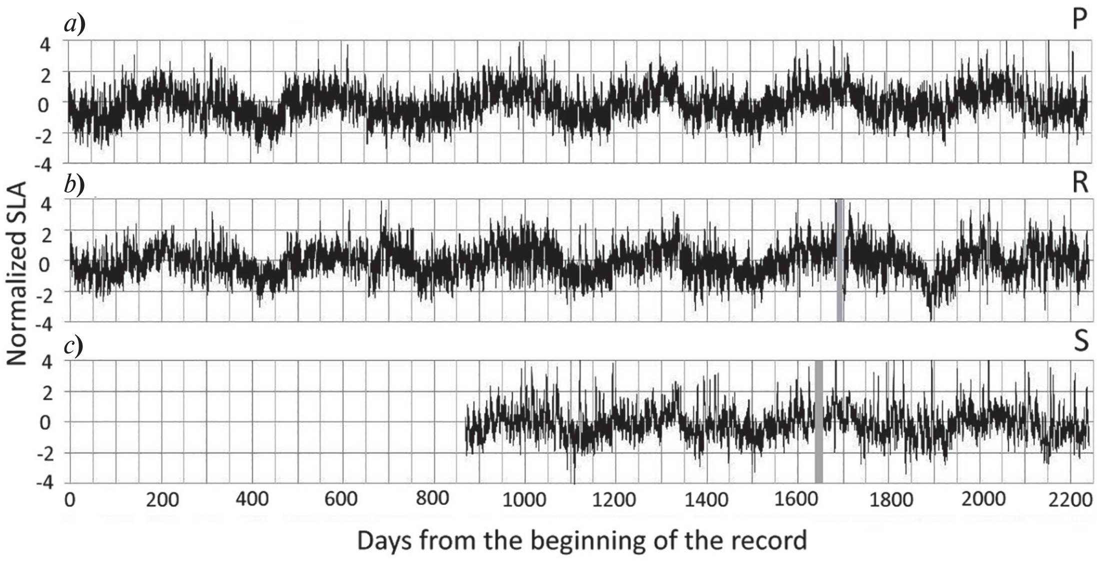


**Fig. 2.** Normalized sea level anomalies (SLA) at stations P (*a*), R (*b*) and S (*c*). Two-week gaps are shown by vertical bars for stations R and S.

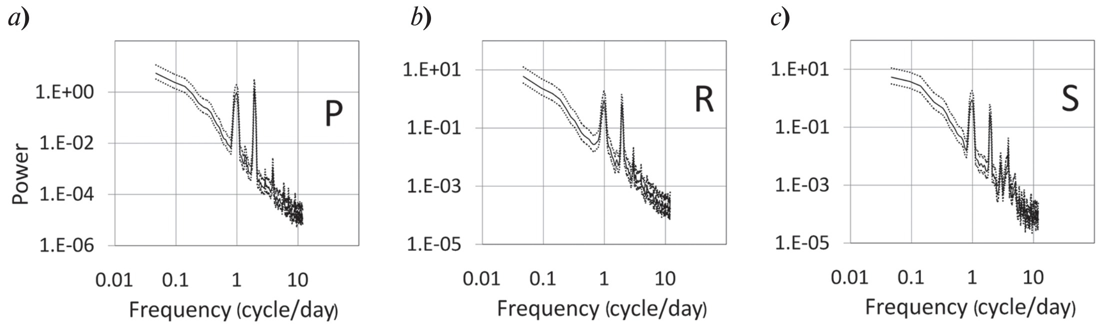


**Fig. 3.** Fourier power spectra of SLA in 2015 at stations P (*a*), R (*b*) and S (*c*).

All the gaps were linearly interpolated and the normalized SLA were computed afterward. Gaps less than 1 day are not significant on timescales beyond the tidal range. However, the two-week gaps in the data at stations R and S are significant and therefore should not be analyzed, as marked by the vertical bars in figs 2 and 4. Additionally, the data were averaged within 2 hours. This is quite sufficient for capturing the considered timescales and simplifies the processing, keeping less than 30000 counts in the time series; it also reduces data errors and removes high frequency fluctuations, including seiches.

The Fourier spectra were computed for the three stations, using the hourly data for 2015, which are the most complete (fig. 3). The spectrum statistical significance was estimated based on the chi-squared distribution. The analysis of non-stationary oscillations was based on the wavelet transform (WT) with the DOG-9 mother wavelet. The frequently used complex Morlet wavelet providing good resolution in the frequency domain produces uninformative spectra, with statistically significant power being mostly confined at the annual timescale. On the contrary, the real wavelets, such as the DOG wavelet, provide good resolution in the time domain, which is important for highly non-stationary signals, while the high (9th) order of the DOG wavelet provides reasonable resolution in the frequency domain, resulting in the informative spectra. It is also important that local WT spectra are reliable outside the two-week interpolated gaps for the data at stations R and S. Both WT diagrams and power spectra ($|WT|^2$) are shown in fig. 4 (see Inset). Timescales were estimated by a number of minimum/maximum pairs on the WT diagrams, while power spectra provide an estimation of statistical significance with respect to the red noise spectra [26]; 90 % confidence level is accepted. The cones of influence (COI) show areas where edge effects become important (fig. 4). The modified Torrence and Compo's procedure [26] was used for WT computation and visualization.

### 3. Results and discussion

As revealed by the WT diagrams and spectra, tide gauge records manifest intense temporal variability on multiple, from tidal to QB timescales (fig. 4, see Inset). The Fourier spectra feature strong, statistically significant diurnal, semi-diurnal, and higher frequency peaks, the latter being the tidal overtones (fig. 3). This pattern is consistent with earlier findings [12, 13]. The intensity of the diurnal peaks is the same at the three stations, while the semi-diurnal peaks weaken from the south to north, i. e. from station P to station S, which is in line with previous findings [13]. There is statistically significant power on the tidal timescales in the WT power spectra as well, with the exception of the semi-diurnal tide for station S where it is the weakest among the three stations (fig. 4, *f*). During several periods, the WT spectral power for station R is significant in the entire 12—24 hour range, implying the intensification of inertial oscillations. (See the 720—770th, 950—1070th, 1330—1450th, 1750—1810th and 2110—2150th days in fig. 4, *d*, which corresponds to 12/22/2011—2/10/2012, 8/8—12/16/2012, 8/23—12/21/2013, 10/17—12/16/2014 and 10/2—11/21/2015). The inertial oscillations can be generated by the strong wind forcing, which occurs in the cold season and also during the tropical cyclone passage in late summer. It is in these periods that the merging of the tidal and inertial timescales was detected.

Annual oscillations are the most intense in the WT spectra, ranging 25—30 cm for stations P and R and 15—20 cm for the northernmost station S (cf. the SLA time series in fig. 2). The seasonal minima occurred in late January to early February and shifted to March at the station S in 2012, while the seasonal maxima occurred in late July to early August and shifted to September at station R in 2011 and 2014. These timings are consistent with earlier findings [1, 2], while minor discrepancies can be attributed to the short record. The QB oscillations are statistically significant in the WT spectra for stations P and R, in line with previous findings from the altimetry data [3, 4], although in the spectrum for station S they are almost absent, probably due to the shorter record (fig. 4, *f*).

The annual WT extremes spread to intra-annual timescales, splitting up to two or three, corresponding to semi-annual and 120–130 day oscillations (fig. 4). These oscillations are non-stationary and can weaken or disappear, for instance from mid July 2011 through early August 2012 (550–950th day from the beginning of the record) for station P or from mid March through mid November 2012 (800–1050th days from the beginning of the record) for station R. The 70–80 day oscillations are also statistically significant and they, in turn, merge together at the 120–130 day and semiannual timescales (fig. 4). The semiannual oscillations are the strongest for station R, resulting in the statistically significant semiannual maximum in the mean (averaged in time) WT spectrum. The 120–130 and 70–80 day oscillations are the strongest for station S, resulting in the statistically significant 126 and 73 day maxima in the mean WT spectrum.

An attempted computation of joint spectra did not provide usable information, as the significant power was confined to the annual timescale. This is because the joint spectra should be computed with the use of the complex Morlet wavelet enabling the estimation of phase shifts between time series, which, in this case, would produce uninformative spectra. Therefore, in order to estimate the relationship between the three stations, SLA time series were band-pass filtered in the 120–130 and 70–80 day ranges.

When the normalized band-pass filtered SLA are strong they exceed 0.15–0.2 (fig. 5) and the corresponding dimensional SLA exceed 1.8–2.7 cm, which is well above the data errors. In both ranges, the three time series closely matched during the most part of the record until late April 2014. (The paired correlations are equal to 0.56–0.80.) The exception is the period from early August 2011 through late June 2012 (580–900th days from the beginning of the record) when the band-pass filtered SLA for stations P and R diverged. This matching pattern implies the same physical origins of these oscillations at the three stations more than 200 km distant from each other. The mismatch near the end of the record (from May 2014, 1580th day from the beginning of the record) can be probably related to specific forcings in the three areas; remarkable are the extremely strong SLA at station R (fig. 5).

The 100–150 day oscillations were detected in the southern Japan Sea and can be explained by the transport variations in the Korea Strait [7]. To the best of our knowledge, strong oscillations on the 120–130 and 70–80 day timescales were not detected in the northwestern Japan Sea, either from tide gauge data, or from satellite altimetry measurements. Therefore, it may be hypothesized that they are related to processes in the northwestern coastal area. This complies with the finding based on data from the autonomous ‘Aqualog’ profiler moored 35 km offshore station P: fluctuations on the 80–110 day timescale were detected in the pycnocline temperature and depth [27]. The ‘Aqualog’ data cover half a year from mid April through mid October 2015, which explains the merging of two timescales detected in the 6 year tide gauge records.

In the range between the tidal and 70–80 day timescales, the sea level oscillations are extremely non-stationary and there is a band of low power between the tidal and longer timescales (fig. 4). In the 2–7 day range, which corresponds to the atmospheric synoptic timescale, the power is low for stations P and R, while it is higher and often statistically significant for station S (fig. 4). This is in line with earlier findings of a storm surge strengthening from the south to the north [14]. In the range between the 2–7 and 70–80 day there are patches of the statistically significant spectral power, which are separated by low power gaps. These patches are shifted in the frequency domain, with the periods (scales) increasing or decreasing in time (fig. 4). This pattern suggests that SLA in this range can represent dynamic structures passing by the stations and these structures can be of different sizes and translational speeds.

The statistically significant spectral power within the considered range is mostly confined between 8 and 40 days and gaps tend to cover the range between 15 and 20 days. The oscillations on the scales larger and smaller than the gaps can be related to mesoscale and submesoscale eddies, respectively, according to their lifetimes [21, 22]. In particular, it was revealed from infrared satellite imagery that shear eddies developing between the Primorye Current and

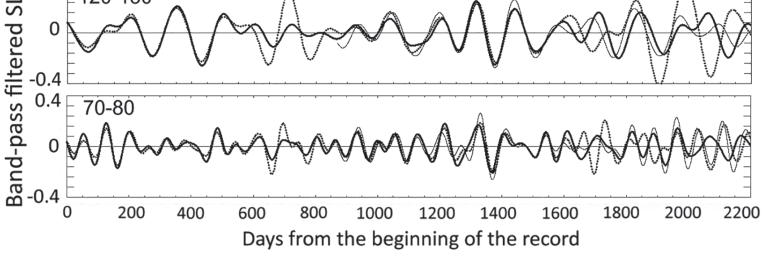


**Fig. 5.** SLA band-pass filtered in the 120–130 and 70–80 day ranges for stations P (thick solid line), R (dashed line), and S (thin solid line).

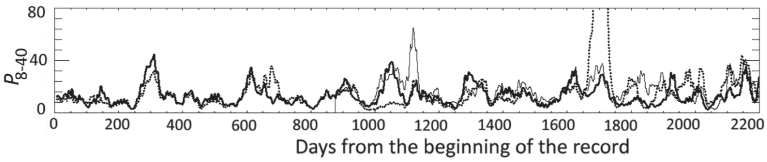


**Fig. 6**. $P_{8-40}$ time series smoothed, with the 15 day window, for stations P (thick solid line), R (dashed line), and S (thin solid line).

the coast are often surrounded by small submesoscale eddies [21]. However, it is difficult to distinguish two kinds of structures from the WT spectra (fig. 4); for this reason, a joint analysis was performed and the WT spectral power was averaged in the 8–40 day range (hereafter denoted as $P_{8-40}$). $P_{8-40}$ was smoothed with the 15 day window filter, removing individual events but facilitating the comparison of variability at the three stations (fig. 6). (Note that similar results were obtained for the ranges between 7–8 and 40–50 day).

An extremely intense $P_{8-40}$ maximum for station R in August — September 2014 (1670–1730th day from the beginning of the record) should not be taken into consideration, as it includes the two-week data gap. (fig. 6 does not include this maximum for the sake of better representation of real variability.) $P_{8-40}$ is very close for the three stations during the period before July 2014 (1640th day from the beginning of the record). (The two exceptions are the periods from mid October through early December 2011, i. e. 650–700th days from the beginning of the record, and from early September through late December 2012, i. e. 980–1090th day). For the period before July 2014, the paired correlations between the $P_{8-40}$ time series are statistically significant: they are equal to 0.62 for stations P and R, 0.58 for stations P and S, and 0.47 for stations R and S. However, the $P_{8-40}$ time series for the three stations diverged in July 2014 (fig. 6). Note that the 120–130 and 70–80 day oscillations diverged in May 2014 (from 1580th day from the beginning of the record; fig. 5), implying the same physical origins for them and $P_{8-40}$.

In order to estimate $P_{8-40}$ timescales of variability, the WT diagram and power spectrum were computed for station P (fig. 7, see Inset), as the most informative due to the best data quality. The statistically significant timescales are QB, annual, 120–130 and 70–80 day, i. e. the same as for SLA. The annual cycle is strong, like for SLA, but rather unstable. The $P_{8-40}$ annual minima and maxima fell on April to May and October to November, respectively, at the beginning of the record. The annual cycle shifted during the period from August 2011 through July 2012 and, as a result, was matching to the SLA annual cycle, with the minima and maxima in late January to early February and late July to early August, respectively. Another shift occurred in late 2014 and both annual cycles became out of phase by August 2015. The unsteady $P_{8-40}$ annual cycle can be explained by the fact that dynamic structures in the station P area are of different origins: they can come from the northeast with the Primorye Current, from the south, southwest or east and are not directly linked to the seasonal sea level variability. The $P_{8-40}$ annual maxima spread to the shorter periods, splitting up at the semiannual, 120–130 day and 70–80 day timescales in the same way as in the SLA spectrum, although the $P_{8-40}$ spectrum is more regular and the linkages between the timescales are more robust (cf. figs. 4 and 7). This similarity implies that the sea level variability on the 120–130 and 70–80 day timescales is related to dynamic mesoscale and submesoscale structures.

The physical nature of the 120–130 and 70–80 day oscillations is not yet clear and requires special investigation. However, some preliminary considerations can be suggested as follows. The non-linear effects in the sea level variability were earlier discussed and they were related to the intense seasonal cycle in the Sea of Japan [3]. In particular, the semi- and quarter-annual oscillations (2 and 4 cycle/year) were considered as the annual cycle overtones and were also shown to be the most intense in the western part of the Sea of Japan [3]. (Note that the 90 day oscillations were statistically significant in the times when the 120–130 and 70–80 maxima were merged in figs. 4, 7.) It was also pointed out that the non-linear interaction of the annual (frequency $w_1 = 1$ cycle/year) and semiannual (frequency $w_2 = 2$ cycles/year) oscillations can generate oscillations of frequency $w_3 = w_1 + w_2 = 3$ cycles/year [3], which approximately corresponds to the 120–130 timescale. Similarly, the 70–80 day oscillations can be considered as close to those at the $w_4 = w_2 + w_3 = 2 + 3 = 5$ cycles/year frequency. (This matching is imperfect, which can be explained by insufficient resolution of the DOG wavelet in the frequency domain.) At any rate, the non-linear effects can explain the interaction of strong oscillations, but this is not always the case (figs. 4, 7).

An origin of the discussed sea level oscillations can also be looked for in dynamic processes: the semiannual oscillations of sea level were explained by the circulation changes in the Sea of Japan forced by wind [3, 16]. However, an important role of the topographic Rossby waves, sometimes called gradient — vorticity waves [28], in the Sea of Japan was earlier suggested, too [3]. In particular, the Rossby waves were engaged to explain the cell structure and SLA movement on the annual and semiannual timescales [29].

The matching (for the most part of the record) or mismatched (at the end of the record) sea level variability on the considered intra-annual timescales in the locations more than 200 km distant from each other implies that the signals do not propagate along the coast but come from the open sea, thus suggesting the forcing from planetary Rossby waves. However, this assumption requires the special investigation and should be a subject of further study.

## 4. Conclusion

Sea level variability was analyzed using tide gauge data for 2010–2015 from three Russian hydrometeorological stations located along the open coastline in the Primorye (Liman) Current zone, the northwestern part of the Sea of Japan. The wavelet transform was applied to elucidate non-stationary oscillations. The QB, annual, semiannual, tidal diurnal and semi-diurnal, and inertial sea level oscillations, which were found in earlier studies, were also detected in the analyzed data.

Non-stationary sea level oscillations on the 120–130 and 70–80 day timescales were detected for the first time in the northwestern part of the Sea of Japan. They were the most regular at the northernmost station S. These oscillations are consistent with the 80–110 day fluctuations detected in the pycnocline temperature and depth based on measurements from the autonomous 'Aqualog' profiler moored in the vicinity of station P in April — October 2015 [27].

The intensity of dynamic processes was estimated from the wavelet spectral power averaged in the 8–40 day range corresponding to lifetimes of mesoscale and submesoscale eddies in the Primorye Current zone. It was found that this intensity varies on the QB, annual, 120–130 and 70–80 day timescales. This implies that the sea level variability on the 120–130 and 70–80 day timescales can be related to dynamic processes.

At the three coastal stations, more than 200 km distant from each other, the newly revealed kinds of intra-annual variability were in phase before mid 2014 and then diverged; their physical sources need yet to be clarified.

## 5. Acknowledgments

The authors thank the anonymous reviewers for valuable comments. We are highly grateful to Ms. R. Rutka and Dr. S. Archer for careful reading and language checking of the paper.

## 6. Funding

The study was carried out as a part of the State Task No. AAAA-A17–117030110042–2 for POI FEB RAS and the Priority Porgram 'Dalniy Vostok' grant No. 18-I-010.

## Литература

1. *Галеркин Л.И.* Непериодические колебания уровня моря // Основные черты геологии и гидрологии Японского моря / Ред. Степанов В.Н. М.: АН СССР, 1961. С. 192–207.
2. *Oh I.S.*, *Rabinovich A.B.*, *Park M.S.*, *Mansurov R.N.* Seasonal sea level oscillations in the East Sea (Sea of Japan) // J. Kor. Soc. Oceanogr. 1993. V. 28. P. 1–16.
3. *Колдунов В.В.*, *Старицын Д.К.*, *Фукс В.Р.* Изменчивость уровня Японского и Охотского морей по данным спутниковых альтиметрических измерений // Дальневосточные моря России: в 4 кн. / Гл. ред. В.А. Акуличев. Кн. 1: Океанологические исследования / Отв. ред. В.Б. Лобанов, В.А. Лучин. М.: Наука, 2007. С. 184–231.
4. *Трусенкова О.О.*, *Каплуненко Д.Д.* Оценка мод изменчивости уровня Японского моря по данным спутниковой альтиметрии // Океанология. 2013. Т. 53, № 3. С. 347–356.
5. *Morimoto A.*, *Yanagi T.* Variability of sea surface circulation in the Japan Sea // J. Oceanogr. 2001. V. 57, N 1. P. 1–13.
6. *Hirose N.*, *Ostrovskii A.G.* Quasi-biennial variability in the Japan Sea // J. Geophys. Res. 2000. V. 105, N 6. P. 14011–14027.
7. *Choi B.-J.*, *Haidvogel D.B.*, *Cho Y.-K.* Nonseasonal sea level variations in the Japan/East Sea from satellite altimeter data // J. Geophys. Res. 2004. V. 109, N12. doi: 10.1029/2004JC002387
8. *Gordon A.I.*, *Giulivi C.* Pacific decadal oscillation and sea level in the Japan/East Sea // Deep Sea Research I. 2004. V. 51, N 5. P. 653–663. . doi: 10.1016/j.dsr.2004.02.005
9. *Kang S.K.*, *Cherniawsky J.Y.*, *Foreman G.G.*, *Min H.S.*, *Kim C.-H.*, *Kang H.-W.* Patterns of recent sea level rise in the East/Japan Sea from satellite altimetry and in situ data // J. Geophys. Res. 2005. V. 110, N C07. doi: 10/1029/2004JC002565
10. *Marcos M.*, *Tsimplis M.N.*, *Calafat F.M.* Inter-annual and decadal sea level variations in the north-western Pacific marginal seas // Progr. Oceanogr. 2012. V. 105. P. 4–21. doi: 10.1016/j.pocean.2012.04.010
11. *Трусенкова О.О.* Долгосрочные изменения уровня Японского моря по данным спутниковых альтиметрических измерений // Исследование Земли из космоса. 2018. № 2. С. 38–47. doi: 10.1134/S0001433818090396

12. *Супранович Т.И.*, *Богданов К.Т.* Часть V. Приливные явления // Гидрометеорология и гидрохимия морей. Т. 8. Японское море. Вып. 1. Гидрометеорологические условия / Ред. Васильев А.С., Терзиев Ф.С., Косарев А.Н. СПб.: Гидрометеоиздат, 2003. С. 257–269.
13. *Rabinovich A.B.*, *Shevchenko G.V.*, *Sokolova S.E.* An estimation of extreme sea levels in the northern part of the Sea of Japan // La Mer. 1992. V. 30. P. 179–190.
14. *Савельев А.В.* О влиянии атмосферного давления и ветра на колебания среднего уровня Японского моря вдоль побережья Приморья // Тр. ДВНИИ. 1983. Вып. 100. С. 83–86.
15. *Фирсов П.Б.*, *Савельев А.В.*, *Ковбас Ю.Д.* Часть VI. Непериодические колебания уровня моря // Гидрометеорология и гидрохимия морей. Т. 8. Японское море. Вып. 1. Гидрометеорологические условия / Ред. Васильев А.С., Терзиев Ф.С., Косарев А.Н. СПб.: Гидрометеоиздат, 2003. С. 269–312.
16. *Трусенкова О.О.* Моделирование региональных особенностей циркуляции Японского моря под различным внешним воздействием // Изв. ТИНРО. 2012. Т. 169. С. 118–133.
17. *Kim T.-K.*, *Yoon J.-H.* Seasonal variation of upper layer circulation in the Northern part of the East/Japan Sea // Continental Shelf Research. 2010. V. 30, N 12. P. 1283–1301. doi: 10.1016/j.csr.2010.04.006
18. *Старицын Д.К.*, *Фукс В.Р.* Сезонная изменчивость уровня Японского моря (по данным альтиметрических измерений) // Вестник СПбГУ. Науки о Земле. 2003. № 4. С. 56–71.
19. *Лобанов В.Б.*, *Пономарев В.И.*, *Салюк А.Н.*, *Тищенко П.Я.*, *Тэлли Л.Д.* Структура и динамика синоптических вихрей северной части Японского моря // Дальневосточные моря России. Кн. 1: Океанологические исследования. М.: Наука, 2007. С. 450–473.
20. *Danchenkov M.A.*, *Lobanov V.B.*, *Riser S.C.*, *Kim K.*, *Takematsu M.*, *Yoon J.-H.* A history of physical oceanographic research in the Japan/East Sea // Oceanogr. 2006. V. 19, N 3. P. 18–31.
21. *Пономарев В.И.*, *Файман П.А.*, *Дубина В.А.*, *Ладыченко С.Ю.*, *Лобанов В.Б.* Синоптическая вихревая динамика над северо-западным материковым склоном и шельфом Японского моря (моделирование и результаты дистанционных наблюдений) // Современные проблемы дистанционного зондирования Земли из космоса. 2011. Т. 8, № 2. С. 100–104.
22. *Ладыченко С.Ю.*, *Лобанов В.Б.* Синоптические вихри в районе залива Петра Великого по спутниковым данным // Исследование Земли из космоса. 2013. № 4. С. 315.
23. *Chelton D.B.*, *Schlax M.G.*, *Samelson R.* Global observations of nonlinear mesoscale eddies // Progress in Oceanography. 2011. V. 91, N 2. P. 167–216.
24. *Lee D.-K.*, *Niiler P.* Surface circulation in the southwestern Japan/East Sea as observed from drifters and sea surface height // Deep-Sea Research I. 2010. V. 57, N10. P. 1222–1232.
25. *Míguez B.M.*, *Tustut L.*, *Wöppelmann G.* Performance of modern tide gauges: towards mm-level accuracy // Advances in Spanish Physical Oceanography / Eds. M. Espino, J. Font, J.L. Pelegrí, A. Sánchez-Arcilla. Barcelona: Instituto de Ciencias del Mar, 2012. P. 221–228.
26. *Torrence C.*, *Compo G.P.* A practical guide to wavelet analysis // Bull. Amer. Meteorol. Soc. 1998. V. 79, № 1. P. 61–78.
27. *Трусенкова О.О.*, *Островский А.Г.*, *Лазарюк А.Ю.*, *Лобанов В.Б.* Характер изменчивости термохалинной структуры вод над континентальным склоном северо-западной части Японского моря у побережья Приморья // Океанологические исследования. 2019. Т. 47, № 3. С. 188–205.
28. *Белоненко Т.В.*, *Захарчук Е.А.*, *Фукс В.Р.* Градиентно-вихревые волны в океане. СПб.: Издательство С.-Петербургского университета, 2004. 215 с.
29. *Зверева А.Е.*, *Фукс В.Р.* Конвергенция потоков в поле градиентно-вихревых волн в котловине Уллын Японского моря // Современные проблемы дистанционного зондирования Земли из космоса. 2016. Т. 13, № 2. С. 25–33. doi: 10.21046/2070–7401–2016–13–2–25–33

## References

1. *Galerkin L.I.* Aperiodic oscillations of sea level. *Osnovnye Cherty Geologii i Gidrologii Yaponskogo Morya*. Ed. Stepanov V.N. *Moscow*, *AN SSSR*, 1961, 192–207 (in Russian).
2. *Oh I.S.*, *Rabinovich A.B.*, *Park M.S.*, *Mansurov R.N.* Seasonal sea level oscillations in the East Sea (Sea of Japan*). J. Kor. Soc. Oceanogr.* 1993, 28, 1–16.
3. *Koldunov V.V.*, *Staritsyn D.K.*, *Fuks V.R.* Variability of sea level in the Japan and Okhotsk Seas by satellite altimetry data. *Dal'nevostochnye Morya Rossii. Kn. 1: Okeanologicheskie Issledovaniya.* Chief ed. Akulitchev V.A., eds. Lobanov V.B., Luchin V.A. *Moscow*, *Nauka*, 2007, 184–231 (in Russian).
4. *Trusenkova O.O.*, *Kaplunenko D.D.* Variability modes of sea level in the Sea of Japan. *Oceanology*. 2013, 53(3), 308–316. doi: 10.1134/S000143701302015X
5. *Morimoto A.*, *Yanagi T.* Variability of sea surface circulation in the Japan Sea. *J. Oceanogr.* 2001, 57(1), 1–13. doi: 10.1023/A:1011149401735

6. *Hirose N., Ostrovskii A.G.* Quasi-biennial variability in the Japan Sea. *J. Geophys. Res.* 2000, 105(6), 14011–14027.
7. *Choi B.-J., Haidvogel D.B., Cho Y.-K.* Nonseasonal sea level variations in the Japan/East Sea from satellite altimeter data. *J. Geophys. Res.* 2004, 109(12). doi: 10.1029/2004JC002387
8. *Gordon A.I., Giulivi C.* Pacific decadal oscillation and sea level in the Japan/East Sea. *Deep Sea Res. I.* 2004, 51(5), 653–663. doi: 10.1016/j.dsr.2004.02.005
9. *Kang S.K., Cherniawsky J.Y., Foreman G.G., Min H.S., Kim C.-H., Kang H.-W.* Patterns of recent sea level rise in the East/Japan Sea from satellite altimetry and in situ data. *J. Geophys. Res.* 2005, 110(C07). doi: 10/1029/2004JC002565
10. *Marcos M., Tsimplis M.N., Calafat F.M.* Inter-annual and decadal sea level variations in the north-western Pacific marginal seas. *Progr. Oceanogr.* 2012, 105, 4–21. doi: 10.1016/j.pocean.2012.04.010
11. *Trusenkova O.O.* Long-term variation in the level of the Sea of Japan based on satellite altimetry measurements. *Izv. Atmos. Ocean. Phys.* 2018, 54(9), 1023–1030. doi: 10.1134/S0001433818090396
12. *Supranovich T.I., Bogdanov K.T.* Part V. Tides. *Gidrometeorologiya i Gidrokhimiya Morei. T. 8. Yaponskoe More. Vyp. 1. Gidrometeorologicheskie Usloviya.* Eds. Vasil'ev A.S., Terziev F.S., Kosarev A.N. *St. Petersburg, Gidrometeoizdat*, 2003, 257–269 (in Russian).
13. *Rabinovich A.B., Shevchenko G.V., Sokolova S.E.* An estimation of extreme sea levels in the northern part of the Sea of Japan. *La Mer.* 1992, 30, 179–190.
14. *Savel'ev A.V.* Impact of atmospheric pressure and winds on fluctuations of the mean sea level in the Japan Sea. *Trudy DVNII.* 1983, 100, 83–86 (in Russian).
15. *Firsov P.B., Savel'ev A.V., Kovbas Yu.D.* Part VI. Non-periodic sea level fluctuations. *Gidrometeorologiya i Gidrokhimiya Morei. T. 8. Yaponskoe More. Vyp. 1. Gidrometeorologicheskie Usloviya.* Eds. Vasil'ev A.S., Terziev F.S., Kosarev A.N. *St. Petersburg, Gidrometeoizdat*, 2003, 269–312 (in Russian).
16. *Trusenkova O.O.* Modeling of regional circulation patterns in the Japan Sea under various forcing scenarios. *Izv. TINRO.* 2012, 169, 118–133 (in Russian).
17. *Kim T.-K., Yoon J.-H.* Seasonal variation of upper layer circulation in the northern part of the East/Japan Sea. *Continental Shelf Research.* 2010, 30(12), 1283–1301. doi: 10.1016/j.csr.2010.04.006
18. *Staritzyn D.K., Foux V.R.* Seasonal variability of the Japan Sea's surface height on altimeter measurements. *Vestnik SPbGU, Seriya 7.* 2003, 4(31), 56–71 (in Russian).
19. *Lobanov V.B., Ponomarev V.I., Salyuk A.N., Tishchenko P. Ya., Talley L.D.* Structure and dynamics of mesoscale eddies in the northern Japan Sea. *Dal'nevostochnye Morya Rossii. Kn. 1: Okeanologicheskie Issledovaniya.* Chief Ed. Akulitchev V.A., eds. Lobanov V.B., Luchin V.A. *Moscow, Nauka*, 2007, 450–473 (in Russian).
20. *Danchenkov M.A., Lobanov V.B., Riser S.C., Kim K., Takematsu M., Yoon J.-H.* A history of physical oceanographic research in the Japan/East Sea. *Oceanogr.* 2006, 19(3), 18–31.
21. *Ponomarev V.I., Faiman P.A., Dubina V.A., Ladychenko S. Yu., Lobanov V.B.* Mesoscale eddy dynamics over the northwest Japan Sea continental slope and shelf (simulation and remote sensing results). *Sovremennye Problemy Distantsionnogo Zondirovaniya Zemli iz Kosmosa.* 2011, 8(2), 100–104 (in Russian).
22. *Ladychenko S. Yu., Lobanov V.B.* Mesoscale eddies in the area of Peter the Great Bay according to satellite data. *Izvestiya, Atmospheric and Oceanic Physics.* 2013, 49, 939–951.
23. *Chelton D.B., Schlax M.G., Samelson R.* Global observations of nonlinear mesoscale eddies. *Progress in Oceanography.* 2011, 91(2), 167–216.
24. *Lee D.-K., Niiler P.* Surface circulation in the southwestern Japan/East Sea as observed from drifters and sea surface height. *Deep Sea Res. I.* 2010, 5710, 1222–1232.
25. *Míguez B.M., Tustut L., Wöppelmann G.* Performance of modern tide gauges: towards mm-level accuracy. *Advances in Spanish Physical Oceanography.* Eds. Espino M., Font J., Pelegrí J.L., Sánchez-Arcilla A. *Barcelona, Instituto de Ciencias del Mar*, 2012, 221–228.
26. *Torrence C., Compo G.P.* A practical guide to wavelet analysis. *Bull. Amer. Meteorol. Soc.* 1998, 79(1), 61–78.
27. *Trusenkova O.O., Ostrovskii A.G., Lazaryuk A. Yu., Lobanov V.B.* Variability of the thermohaline structure at the continental slope off the Russian coast, the northwestern Japan Sea. *Journal of Oceanological Research.* 2019, 47(3), 188–205 (in Russian).
28. *Belonenko T.V., Zakharchuk E.A., Fuks V.R.* Gradient — vorticity waves in the ocean. *St. Petersburg, St. Petersburg University Publishing House*, 2004, 215 p. (in Russian).
29. *Zvereva A.E., Fuks V.R.* Flux convergence in gradient — vorticity waves in the Tsushima/Ulleung Basin, the Japan/East Sea. *Sovremennye Problemy Distantsionnogo Zondirovaniya Zemli iz Kosmosa.* 2016, 13(2), 25–33 (in Russian). doi: 10.21046/2070–7401–2016–13–2–25–33

К статье *Трусенкова О.О., Лобанов В.Б., Примачев Е.В.* Внутригодовая изменчивость уровня Японского моря в северо-западной прибрежной зоне

*Trusenkova O.O., Lobanov V.B., Primachev E.V.* Sea level intra-annual variability in the coastal north-western part of the Sea of Japan

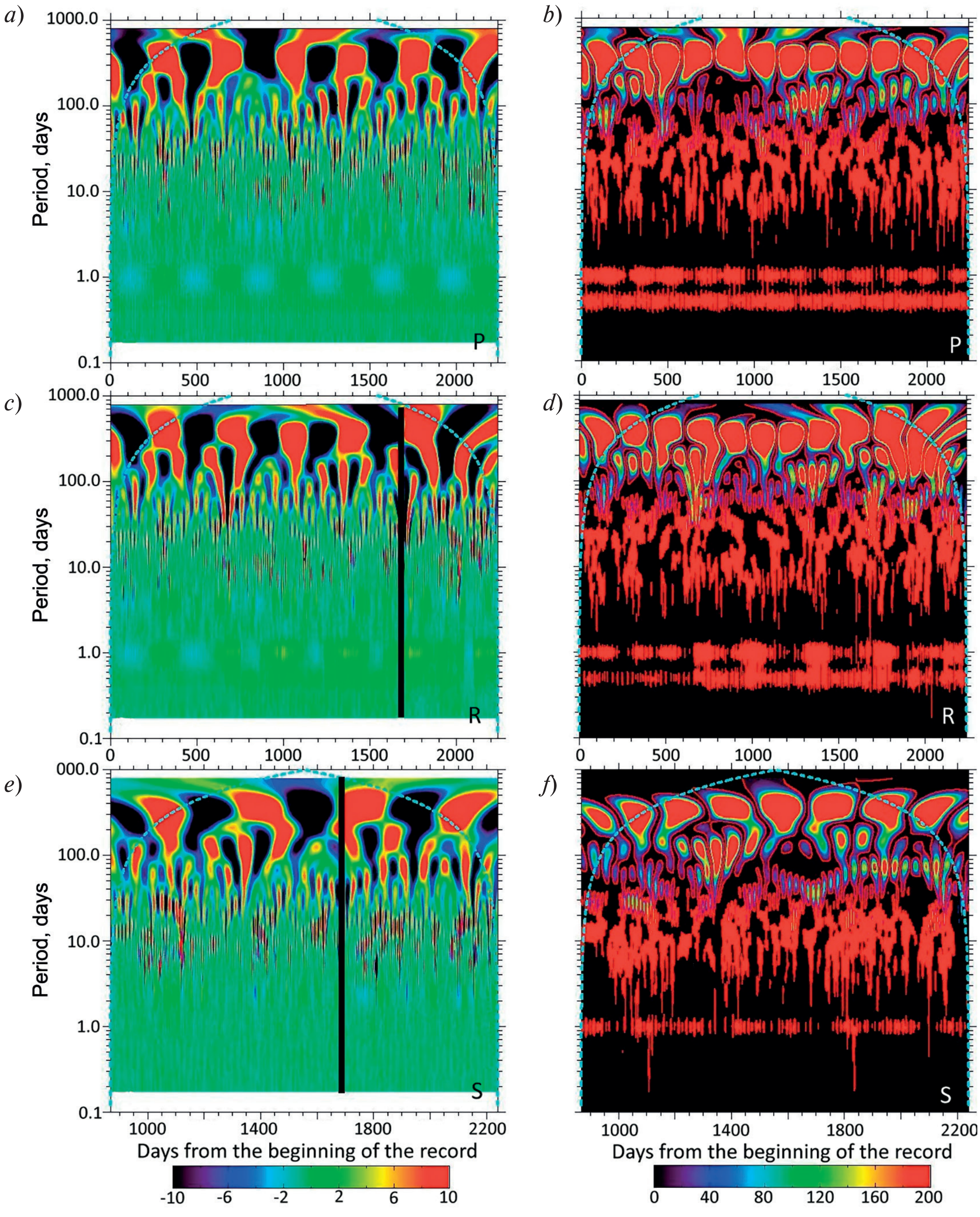


**Fig. 4.** Wavelet transform (WT) diagrams (*a*, *c*, *e*) and power spectra (*b*, *d*, *f*) of SLA at stations P (*a*, *b*), R (*c*, *d*), and S (*e*, *f*). Light-blue dashed lines denote cones of influence (COI). Solid red lines are 90 % confidence levels with respect to the red noise spectra. Vertical bars indicate the two-week gaps for stations R and S.

К статье *Трусенкова О.О., Лобанов В.Б., Примачев Е.В.* Внутригодовая изменчивость уровня Японского моря в северо-западной прибрежной зоне

*Trusenkova O.O., Lobanov V.B., Primachev E.V.* Sea level intra-annual variability in the coastal north-western part of the Sea of Japan

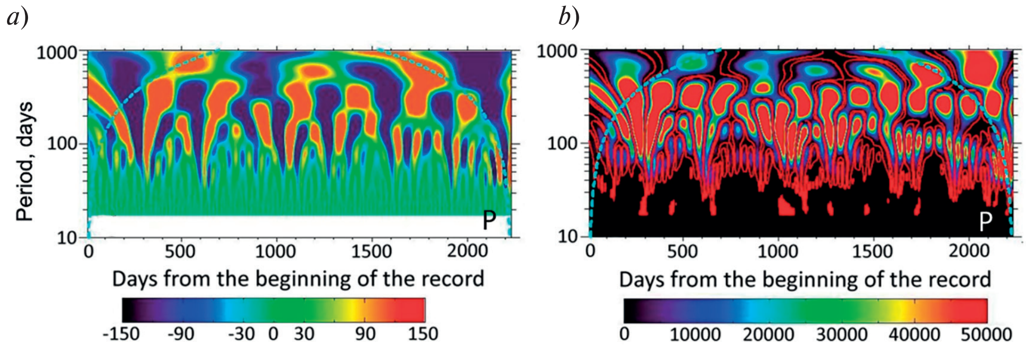


**Fig. 7**. WT diagram (*a*) and power spectrum of $P_{8-40}$ (*b*) for station P. Light-blue dashed lines indicate COI. Solid red lines are 90 % confidence levels with respect to the red noise spectrum.